Journal of Intelligent and Robotic Systems **30:** 267–277, 2001.

Localization of an Autonomous Mobile Robot Based on Ultrasonic Sensory Information

CHIA-JU WU
Department of Electrical Engineering, National Yunlin University of Science & Technology, Touliu, Yunlin 640, Taiwan, R.O.C.; e-mail: wucj@pine.yuntech.edu.tw

CHING-CHIH TSAI
Department of Electrical Engineering, National Chung-Hsing University, Taichung 402, Taiwan, R.O.C.

(Received: 2 November 1999; in final form: 7 June 2000)

Abstract. Based on ultrasonic sensory information, an approach is proposed for localization of autonomous mobile robot (AMRs). In the proposed method, it will be proven that the combination of three ultrasonic transmitters and two receivers can determine both the position and the orientation of an AMR with respect to a reference frame uniquely. In this manner, since only ultrasonic sensors are used, the proposed method will be highly cost-effective and easy to implement. To show the validity and feasibility of the proposed method, the hardware configuration and a series of experiments will be given for illustration.

Key words: localization, autonomous mobile robots, ultrasonic sensors.

1. Introduction

When an autonomous mobile robot performs tasks such as free-range path tracking and reactive navigation, the capability to estimate its position with respect to a reference frame is very important. Among the existing location techniques, most wheeled mobile robots use the *dead-reckoning* method to calculate their current locations. However, since this method is based on the encoded or odometric information from the wheels, it is subject to major accumulation errors caused by wheel slippage or surface roughness. Therefore, the robot may fail to keep track of its true location over long distances.

To compensate for the inaccuracy of dead-reckoning, Kim and Seong [6] devised a highly cost-effective location system which used an encoded magnetic compass to account for abnormal orientation drift due to wheel slippage, thereby resulting in robot position recovery. However, a magnetic compass does not function well at a place where the magnetic field varies from position to position. On the other hand, Song and Suen [11] used Kalman filtering to investigate how a low-cost rate-gyro can be applied to adjust dead-reckoning estimates to overcome the wheel slippage problem. Unfortunately, the low-cost rate-gyro usually suffers from high drift rate and cannot eliminate the cumulative errors caused by surface roughness.

Ultrasonic ranging sensors have proved to be very useful, economical external sensing systems for localization of mobile robots. The numerous ultrasonic location methods can be divided into two groups of technical methodologies. The first one is that the robot measures time-of-flight (TOF) data from itself to its surroundings by using several ultrasonic sensors mounted on itself and then processes this information to obtain its spatial location by means of barrier tests [2], extended Kalman filtering with environment models [7, 8, 10, 12], fuzzy fusion logic [9], and neural networks [5]. The second methodology is based on active beacon positioning, called 3D-location technique [3], which has a transmitter, as a beacon, mounted on the robot and several receivers installed at the prespecified locations with respect to a reference frame. This approach requires the least-squares algorithm or the EKF-based algorithm for converting the TOF temporal data between the beacon and those receivers to the robot location. Generally speaking, robot location techniques based on the first methodology lack accuracy and flexibility. For the 3D-location technique, though the strengths of the system are accurate, how to determine the orientation (heading angle) of the robot is not taken into account.

In the method proposed by one of the authors [13], a novel location system was developed which consists of an improved multisensorial dead-reckoning subsystem and a modified ultrasonic location subsystem. The novelty of the multisensorial dead-reckoning lies in the statistical treatment of the robot's heading readings from a rate-gyro, a magnetic compass, and encoded information from the driving wheels. The features for the ultrasonic system hinge on its strengths, which not only encompass all of the inherent advantages declared in [3] but also provide a simpler, more economical structure for implementation, installation, and use.

Though the method in [13] has the above-mentioned advantages, it should be noted that the ultrasonic sensors are used to determine the position of the robot only, not including the orientation. In this case, one may wonder whether it is possible to determine the position and the orientation of the robot based on ultrasonic sensory information only. This in turn motivates the research in this paper and a novel location method is proposed. In this method, it will be proved first that an ultrasonic transmitter cannot determine both the position and the orientation of an AMR regardless of the number of the ultrasonic receivers. This explains why the determination of orientation is not taken into account in [3] and a magnetic compass is used in [13]. Then it is proved that the combination of three ultrasonic transmitters and two receivers can determine both the position and the orientation of an AMR uniquely provided that the ultrasonic sensors are installed at locations as specified in the proposed method. In this manner, since only ultrasonic sensors are used, it is expected that the proposed system will be highly cost-effective and easy to implement. Moreover, the least-squares algorithm will also be used to process the measured TOF data to obtain a more accurate estimation. To confirm the validity and feasibility of the proposed method, a series of examples will be given for illustration.

The remaining sections of this paper are organized as follows. Section 2 shows the mathematical frame of the location system, in which two theorems are given to determine the minimal number of ultrasonic sensors and the locations to install these sensors. According to these two theorems, Section 3 describes the hardware configuration of the location system. Several experiments will be performed in Section 4 to confirm the accuracy and performance of the proposed method. Discussions and conclusions of the paper are given in Section 5.

2. Mathematical Frame of the Location System

Before showing the hardware configuration of the location system, the minimal number of ultrasonic transmitters and receivers needed in the location system must be determined first. Moreover, the locations to install these sensors also need to be specified. Therefore, some notations will be introduced and two theorems will be given.

Let $\{A\}$ and $\{B\}$ be two frames in a working space. For a point in the space, the representations of this point with respect to the two frames will be denoted as ${}^{A}[x, y, z]$ and ${}^{B}[x, y, z]$, respectively, where the leading superscripts A and B are used to indicate the frame to which the point is referenced. Then if the so-called *homogeneous coordinate representation* [1] is used, one will obtain

$$
{}^{A}\begin{bmatrix} x \\ y \\ z \\ 1 \end{bmatrix} = {}^{A}T_{B} \cdot {}^{B}\begin{bmatrix} x \\ y \\ z \\ 1 \end{bmatrix}, \tag{1}
$$

where ${}^{A}T_{B} \in \mathbb{R}^{4\times 4}$ is the *transform matrix* [1] between frames $\{A\}$ and $\{B\}$.

With the notations in (1), the following two theorems can be obtained.

THEOREM 1. *Suppose that there are two frames $\{A\}$ and $\{B\}$ in a working space. For a given set of m points, let d_i, $i = 1, 2, \ldots, m$, denote the distances of the m points to the origin of frame $\{A\}$. Then from the values of d_i, $i = 1, 2, \ldots, m$, and the representations of the m points with respect to frame $\{B\}$, ${}^{B}[x_i, y_i, z_i]$, $i = 1, 2, \ldots, m$, one cannot determine the transform matrix ${}^{A}T_{B}$ uniquely regardless of the value of m.*

Proof. For convenience of illustration, ${}^{B}[x_i, y_i, z_i]$, $i = 1, 2, \ldots, m$, and d_i, $i = 1, 2, \ldots, m$ will be depicted as shown in Figure 1. From this figure, it is easy to find that if frame $\{B\}$ and the m points are grouped together and then be rotated about the Z_A-axis by a degree of θ, $0 \leqslant \theta \leqslant 2\pi$, then the representations ${}^{B}[x_i, y_i, z_i]$, $i = 1, 2, \ldots, m$, and the values of d_i, $i = 1, 2, \ldots, m$, will keep the same regardless of the value of θ. However, for a different choice of θ the rotation will generate a different transform matrix. Therefore, the transform matrix ${}^{A}T_{B}$

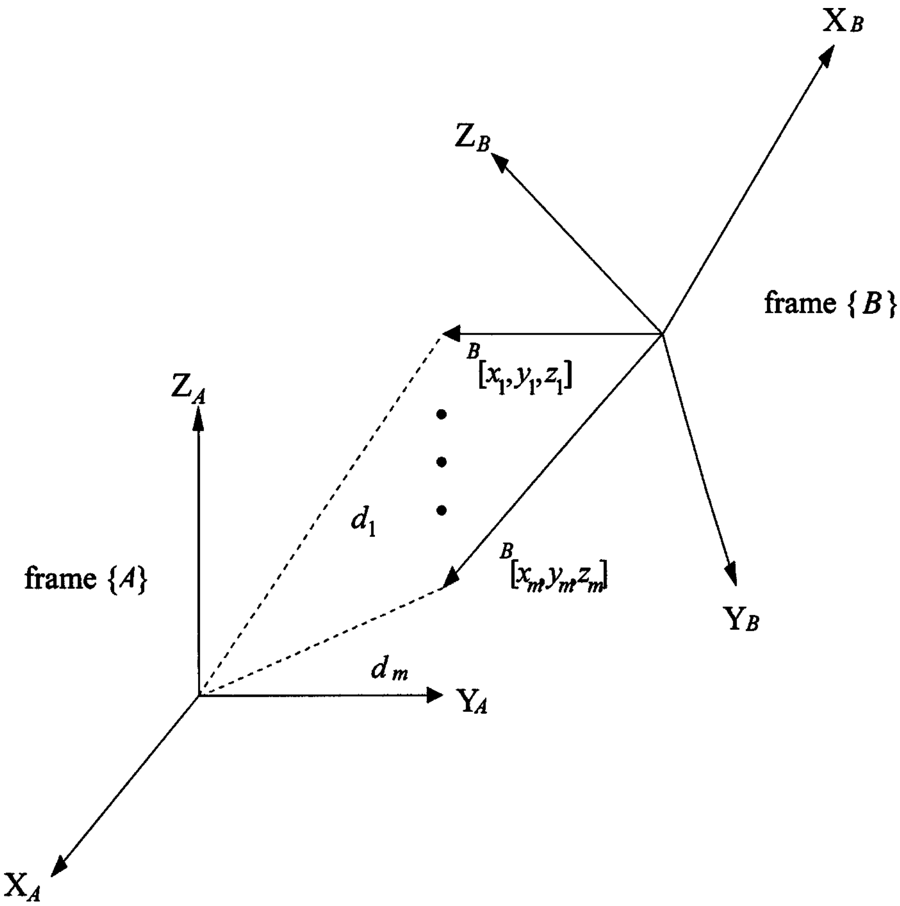

Figure 1. A given set of m points, in which d_i, $i = 1, 2, \ldots, m$, denote the distances of the m points to the origin of frame $\{A\}$ and ${}^B[x_i, y_i, z_i]$, $i = 1, 2, \ldots, m$, are the representations of the m points with respect to frame $\{B\}$.

cannot be determined uniquely from the values of d_i, $i = 1, 2, \ldots, m$, and the representations ${}^B[x_i, y_i, z_i]$, $i = 1, 2, \ldots, m$, regardless of the value of m. □

From the above theorem, one can find easily that the position and the orientation of an AMR cannot be determined uniquely if an ultrasonic transmitter is installed at a specified position of the reference frame and m receivers are mounted on the AMR. This explains why the orientation problem is not discussed in [3] and why a magnetic compass is used in [13]. To determine the position and the orientation of an AMR uniquely, the following theorem will be needed.

THEOREM 2. *Suppose that three points,* $[0, 0, 0]$, $[a, 0, 0]$, *and* $[0, a, 0]$, *are given in a working space, where* a *is a nonzero real number that can be chosen arbitrarily. Then for any two points,* $[x_1, y_1, z]$ *and* $[x_2, y_2, z]$, *in the space, the* *values of* x_1, y_1, x_2, *and* y_2 *can be determined provided that the distances of these two points to the points* $[0, 0, 0]$, $[a, 0, 0]$, *and* $[0, a, 0]$ *are given. This in turn will determine the angle* $\theta = \mathrm{Atan2}(y_2 - y_1, x_2 - x_1)$, *which is a two-argument arc tangent function* [1]. *Meanwhile, the value* z *can also be determined provided that its sign (greater or smaller then zero) is given.*

Proof. Let d_1, d_2, and d_3 denote the distances of the point $[x_1, y_1, z]$ to the points $[0, 0, 0]$, $[a, 0, 0]$, and $[0, a, 0]$, respectively. Then one will obtain

$$x_1^2 + y_1^2 + z^2 = d_1^2, \tag{2}$$

$$(x_1 - a)^2 + y_1^2 + z^2 = d_2^2, \tag{3}$$

$$x_1^2 + (y_1 - a)^2 + z^2 = d_3^2. \tag{4}$$

Subtracting (3) and (4) from (2), respectively, will give

$$2ax_1 - a^2 = d_1^2 - d_2^2 \tag{5}$$

and

$$2ay_1 - a^2 = d_1^2 - d_3^2. \tag{6}$$

Rearranging (5) and (6) will result in

$$x_1 = \frac{d_1^2 - d_2^2 + a^2}{2a} \tag{7}$$

and

$$y_1 = \frac{d_1^2 - d_3^2 + a^2}{2a}. \tag{8}$$

In a similar way, the values of x_2 and y_2 can also be determined. Therefore, the values of x_1, y_1, x_2, and y_2 are determined. Substituting these values into the Atan2 function will then determine the angle $\theta = \mathrm{Atan2}(y_2 - y_1, x_2 - x_1)$. Moreover, substituting the values of x_1 and y_1 into (2) will give

$$z = \pm\sqrt{d_1^2 - x_1^2 - y_1^2}. \tag{9}$$

Therefore, provided that its sign is given, the value of z can be determined from one of the two possible values in (9).

3. Hardware Configuration

The physical configuration of the proposed location system is shown in Figure 2, in which three ultrasonic transmitters are installed at positions $[0, 0, 0]$, $[a, 0, 0]$, and $[0, a, 0]$ of the reference frame, respectively, and two receivers are mounted on the AMR. The only requirement is that the two receivers must be installed at the same height along the z-axis.

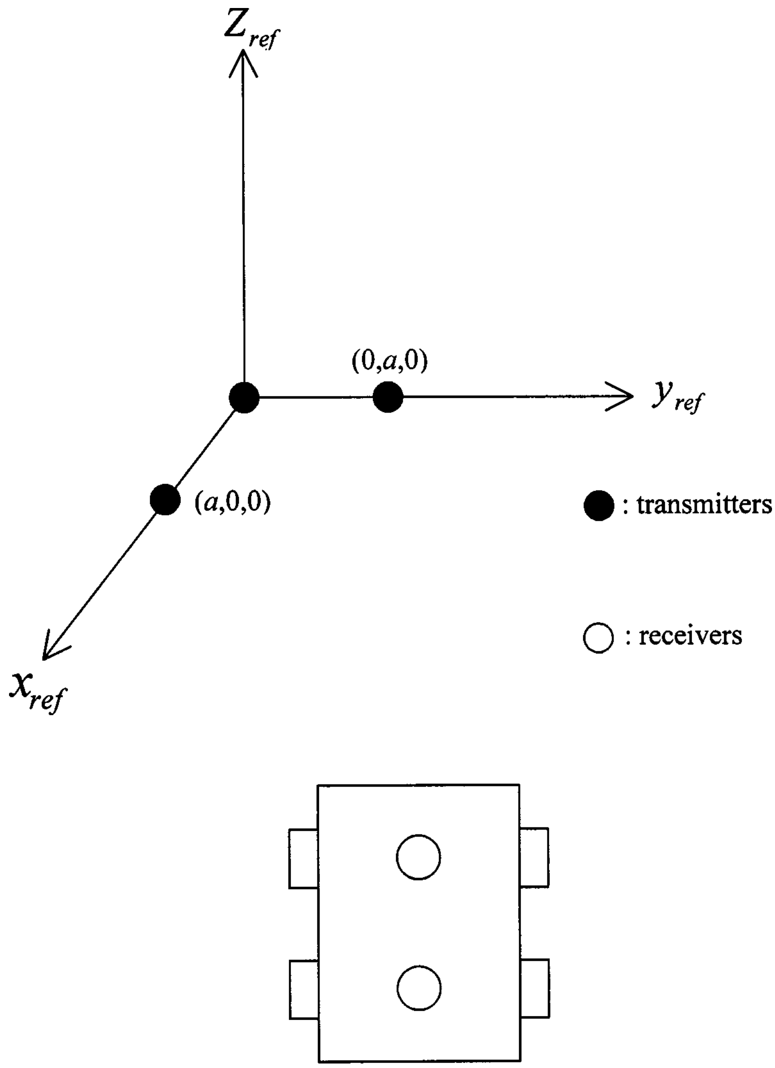

Figure 2. Physical configuration of the proposed system, in which three ultrasonic transmitters are installed at positions [0, 0, 0], [a, 0, 0], and [0, a, 0] of the reference frame, respectively, and two receivers are mounted on the AMR.

In addition to the three transmitter modules and the two receiver modules, the hardware of the location system also contains a pair of RF controlled switches and two 8051 single-chip micro-controllers as depicted in Figure 3. In measuring the distance between the ith transmitter, $1 \leqslant i \leqslant 3$, and the jth receiver, $1 \leqslant j \leqslant 2$, the first RF controlled switch will send a radio signal to the second and the 8051 micro-controller will start the counting of the TOF. Once the second RF controlled switch receives the radio signal, the ith transmitter module will send ultrasonic pulses back to the jth receiver module immediately. In this manner, if the distance

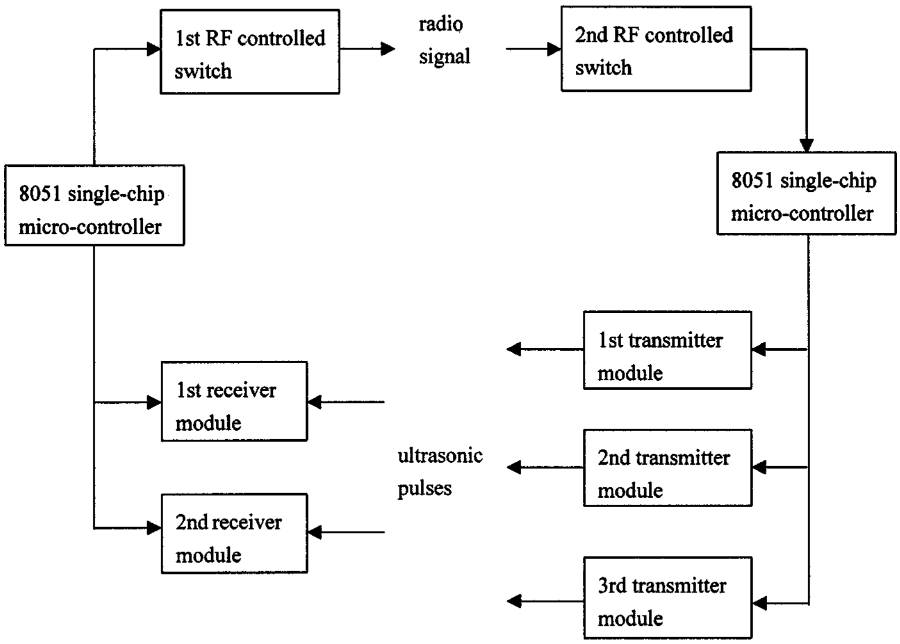

Figure 3. Block diagram of the hardware of the location system.

between the ith transmitter and the jth receiver is denoted by d_{ij}, then one will obtain

$$\mathrm{TOF}_{ij} = \frac{d_{ij}}{V_\mathrm{E}} + \frac{d_{ij}}{V_\mathrm{U}}, \tag{10}$$

where TOF_{ij} is the TOF between the ith transmitter and the jth receiver, and V_E and V_U denote the speeds of the electromagnetic wave and the ultrasonic wave, respectively. However, since V_E is much larger then V_U in practice, (10) can be further simplified to be

$$\mathrm{TOF}_{ij} = \frac{d_{ij}}{V_\mathrm{U}}. \tag{11}$$

Performing the above procedure repeatedly, the values of d_{ij}, $1 \leqslant i \leqslant 3$, $1 \leqslant j \leqslant 2$, will be determined sequentially. With these distances, the position and the orientation of the AMR can then be determined uniquely according to Theorem 2.

4. Experimental Results

Two sets of experimental studies will be performed in this section to investigate the feasibility, accuracy, and performance of the proposed location system. While performing the experiments, the room temperature is 27°C and the counting rate of the 8051 chip is 50 kHz. In the experiments, the three transmitters will be installed

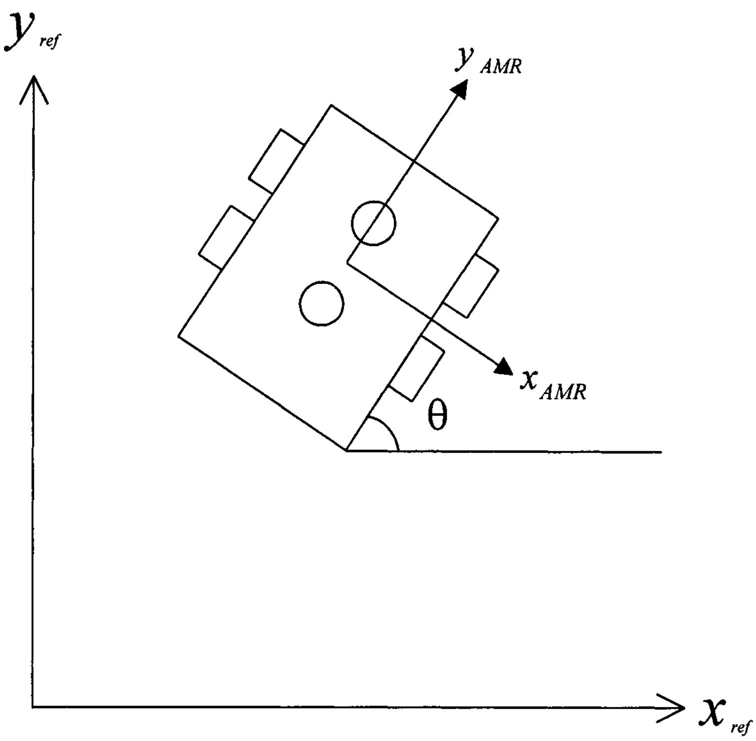

Figure 4. Definitions of the frame {AMR} and the heading angle θ. For convenience of illustration, the axes Z_{ref} and Z_{AMR} are not shown and can be determined according to $Z_{\text{ref}} = X_{\text{ref}} \times Y_{\text{ref}}$ and $Z_{\text{AMR}} = X_{\text{AMR}} \times Y_{\text{AMR}}$, where $\times$ denotes the cross product of two vectors.

at positions [0, 0, 0], [20, 0, 0], and [0, 20, 0] (unit: cm), respectively, with respect to a reference frame. On the other hand, the two receivers will be installed at positions [0, 20, 0] and [0, −20, 0] (unit: cm), respectively, with respect to the frame {AMR}, which is a frame that is attached to the AMR as depicted in Figure 4. The goal of the experiments is to determine the representation of the origin of frame {AMR} with respect to the reference frame and the heading angle θ of the AMR. In each set of experiments, different positions and orientations of the AMR will be given for comparison.

In applying the proposed method, the concept of least-squares method [4] will also be used to increase the accuracy of estimation. The procedure is to apply the proposed method n times first to obtain n sets of measured values, $[x(i), y(i), z(i)]$ and $\theta(i)$, $i = 1, 2, \ldots, n$. Then the optimal estimates of $[x, y, z]$ and θ, which will be denoted by $[\hat{x}, \hat{y}, \hat{z}]$ and $\hat{\theta}$, can be determined by minimizing the total least squares error

$$E = \sum_{i=1}^{n} \left[\left(\hat{x} - x(i)\right)^2 + \left(\hat{y} - y(i)\right)^2 + \left(\hat{z} - z(i)\right)^2 + \left(\hat{\theta} - \theta(i)\right)^2 \right]. \tag{12}$$

Table I. Experimental results of Example 1. By applying the proposed method 10 times, one can obtain 10 sets of measured values, $[x(i), y(i), z(i)]$ and $\theta(i)$, $i = 1, 2, \dots, 10$. The optimal estimates $[\hat{x}, \hat{y}, \hat{z}]$ and $\hat{\theta}$ are then determined from Equations (13)–(16) with $n = 10$.

	Expt. 1	Expt. 2	Expt. 3	Expt. 4
$[x, y, z]$	[0, 0, −190] cm	[0, 0, −190] cm	[0, 0, −190] cm	[0, 0, −190] cm
θ	0°	45°	90°	135°
$\hat{x}$	−3.1 cm	−3.55 cm	−2.87 cm	−1.73 cm
$\hat{y}$	−2.29 cm	−2.92 cm	−1.09 cm	−2.74 cm
$\hat{z}$	−189.02 cm	−188.61 cm	−189.38 cm	−189.3 cm
$\hat{\theta}$	0.6°	46.6°	91.2°	136.71°
$\max_i \lvert\hat{x} - x(i)\rvert$	5.46 cm	3.94 cm	3.75 cm	2.37 cm
$\max_i \lvert\hat{y} - y(i)\rvert$	3.07 cm	5.21 cm	1.31 cm	5.42 cm
$\max_i \lvert\hat{z} - z(i)\rvert$	1.34 cm	1.46 cm	0.79 cm	1.05 cm
$\max_i \lvert\hat{\theta} - \theta(i)\rvert$	0.77°	2.81°	0.82°	2.97°

By setting

$$\frac{\partial E}{\partial \hat{x}} = 0, \qquad \frac{\partial E}{\partial \hat{y}} = 0, \qquad \frac{\partial E}{\partial \hat{z}} = 0, \quad \text{and} \quad \frac{\partial E}{\partial \hat{\theta}} = 0,$$

one will obtain the optimal estimates of $[x, y, z]$ and θ as follows:

$$\hat{x} = \frac{\sum_{i=1}^{n} x(i)}{n}, \tag{13}$$

$$\hat{y} = \frac{\sum_{i=1}^{n} y(i)}{n}, \tag{14}$$

$$\hat{z} = \frac{\sum_{i=1}^{n} z(i)}{n}, \tag{15}$$

$$\hat{\theta} = \frac{\sum_{i=1}^{n} \theta(i)}{n}. \tag{16}$$

EXAMPLE 1. Four experiments will be given in this example, in which the heading angle θ of the AMR are 0°, 45°, 90°, and 135°, respectively. The position of the AMR will be the same in these four experiments and is represented as [0, 0, −190] (unit: cm) with respect to the reference frame. The measuring procedure is to apply the proposed method 10 times first to obtain 10 sets of measured values, $[x(i), y(i), z(i)]$ and $\theta(i)$, $i = 1, 2, \dots, 10$. Then these data are used to determine the optimal estimates $[\hat{x}, \hat{y}, \hat{z}]$ and $\hat{\theta}$ according to (13)–(16). The details of the estimation are given as shown in Table I.

Table II. Experimental results of Example 2. By applying the proposed method 10 times, one can obtain 10 sets of measured values, $[x(i), y(i), z(i)]$ and $\theta(i)$, $i = 1, 2, \ldots, 10$. The optimal estimates $[\hat{x}, \hat{y}, \hat{z}]$ and $\hat{\theta}$ are then determined from Equations (13)–(16) with $n = 10$.

	Expt. 1	Expt. 2	Expt. 3	Expt. 4
$[x, y, z]$	[0, 0, −150] cm	[0, 0, −150] cm	[0, 0, −150] cm	[0, 0, −150] cm
θ	0°	45°	90°	135°
$\hat{x}$	−0.94 cm	−1.48 cm	−1.95 cm	−0.92 cm
$\hat{y}$	−0.47 cm	−1.48 cm	−0.97 cm	−0.52 cm
$\hat{z}$	−149.83 cm	−149.36 cm	−149.30 cm	−149.84 cm
$\hat{\theta}$	0.5°	46.12°	89.22°	136.08°
$\max_i \lvert\hat{x} - x(i)\rvert$	1.02 cm	2.94 cm	3.05 cm	1.43 cm
$\max_i \lvert\hat{y} - y(i)\rvert$	0.81 cm	1.71 cm	1.13 cm	0.73 cm
$\max_i \lvert\hat{z} - z(i)\rvert$	0.19 cm	1.20 cm	0.82 cm	0.34 cm
$\max_i \lvert\hat{\theta} - \theta(i)\rvert$	0.81°	1.46°	0.95°	1.77°

EXAMPLE 2. This example is the same as Example 1 except that the position of the AMR is placed at [0, 0, −150] (unit: cm) with respect to the reference frame. By applying the same measuring procedure as described in Example 1, the optimal estimates $[\hat{x}, \hat{y}, \hat{z}]$ and $\hat{\theta}$ can be determined. The details of the estimation are given as shown in Table II.

5. Discussions and Conclusions

This paper has developed a novel location system for an AMR in a 3D environment based on ultrasonic sensory information only. The hardware of the system consists of three transmitter modules, two receiver modules, a pair of radio control switches, and two 8051 single-chip micro-controllers. Using this system, one can determine the position and the orientation of an AMR uniquely provided that the transmitters and the receivers are installed at locations specified by the proposed theorem.

From the experimental results in Tables I and II, one can find that the estimates in Example 2 are more accurate than those in Example 1. An explanation for this phenomenon is that the distances between the transmitters and the receivers in Example 2 are shorter than those in Example 1. Though the accuracies in both examples are different, the optimal position and orientation estimates of the AMR are all very close to the actual values, which verifies that the proposed system provides highly accurate and reliable estimates.

In performing the experiments, it should be pointed out that only the room temperature is measured. Therefore, one can increase the accuracy of the proposed method by measuring the mean ambient temperature correctly. Moreover, the counting rate the micro-controllers can also be increased for more accurate estimates.

Acknowledgement

This work was supported in part by the National Science Council, Taiwan, R.O.C., under grants NSC88-2213-E-224-035 and NSC88-2213-E-224-037.

References

1. Craig, J. J.: *Introduction to Robotics: Mechanics and Control*, 2nd edn, Addison-Wesley, Reading, MA, 1989.
2. Drumheller, M.: Mobile robot location using sonar, *IEEE Trans. Pattern Analysis Mach. Intelligence* **9** (1987), 325–332.
3. Figueroa, F. and Mahajan, A.: A robust navigation system for autonomous vehicles using ultrasonics, *Control Engrg. Practice* **2** (1994), 49–59.
4. Gerald, C. F. and Wheatley, P. O.: *Applied Numerical Analysis*, 4th edn, Addison-Wesley, Reading, MA, 1989.
5. Janet, J. A., Gutierrez, R., Chase, T. A., White, M. W., and Sutton, J. C.: Autonomous mobile robot global self-localization using Kohonen and region-feature neural networks, *J. Robotic Systems* **14** (1997), 263–282.
6. Kim, J. H. and Seong, P. H.: Experiments on orientation recovery and steering of an autonomous mobile robot using encoded magnetic compass disc, *IEEE Trans. Instrumentation Measurement* **45** (1996) 271–274.
7. Leonarand, J. J. and Durrant-Whyte, H. F.: *Directed Sonar Sensing for Mobile Robot Navigation*, Kluwer, Dordrecht, 1992.
8. Maksarov, D. and Durrant-Whyte, H.: Mobile vehicle navigation in unknown environments: A multiple hypothesis approach, *IEE Proc. Control Theory Appl.* **142** (1995), 385–400.
9. Piasecki, M.: Mobile robot localization by fuzzy logic fusion of multi-sensor data, *Robotics Autonom. Systems* **12** (1994), 155–162.
10. Sabatini, A. M.: A digital signal processing technique for compensating ultrasonic sensors, *IEEE Trans. Instrumentation Measurement* **44** (1995), 869–874.
11. Song, K. T. and Suen, Y. H.: Design and implementation of a path tracking controller with the capacity of obstacle avoidance, in: *Proc. of 1996 Automatic Control Conference*, Taipei, Taiwan, 1996, pp. 134–139.
12. Triggs, B.: Model-based sonar location for mobile robots, *Robotics Autonom. Systems* **12** (1994), 173–186.
13. Tsai, C. C.: A localization system of a mobile robot by fusing dead-reckoning and ultrasonic measurements, *IEEE Trans. Instrumentation Measurement* **47** (1998), 1399–1404.